International Journal of Applied Research in Mechanical Engineering

Volume 1 | Issue 1 Article 13

July 2011

Vibration characteristics of nanocomposite plates under thermal conditions including nonlinear effects

A. Shooshtari
Mechanical Engineering Department, Bu-Ali Sina University, 65175 Hamedan, Iran,
ashooshtari@yahoo.co.in

M. Rafiee
Mechanical Engineering Department, Bu-Ali Sina University, 65175 Hamedan, Iran, m_rafiee@gmail.com

Follow this and additional works at: https://www.interscience.in/ijarme

 Part of the Aerospace Engineering Commons, and the Mechanical Engineering Commons

Recommended Citation

Shooshtari, A. and Rafiee, M. (2011) "Vibration characteristics of nanocomposite plates under thermal conditions including nonlinear effects," *International Journal of Applied Research in Mechanical Engineering*: Vol. 1 : Iss. 1 , Article 13.
DOI: 10.47893/IJARME.2011.1012
Available at: https://www.interscience.in/ijarme/vol1/iss1/13

This Article is brought to you for free and open access by the Interscience Journals at Interscience Research Network. It has been accepted for inclusion in International Journal of Applied Research in Mechanical Engineering by an authorized editor of Interscience Research Network. For more information, please contact sritampatnaik@gmail.com.

Vibration characteristics of nanocomposite plates under thermal conditions including nonlinear effects

A. Shooshtari, M. Rafiee*
Mechanical Engineering Department, Bu-Ali Sina University, 65175 Hamedan, Iran

Abstract : Thermo-mechanical dynamic characteristics of SWCNT-Reinforced Composite Plates are studied in this paper. The material properties of SWCNTs are assumed to be temperature-dependent and are obtained from molecular dynamics simulations. The material properties of carbon nanotube-reinforced composites (CNTRCs) are assumed to be uniform in the thickness direction, and are estimated through a micromechanical model. Based on the multi-scale approach, numerical illustrations are carried out for CNTRC plates and uniformly distributed CNTRC plates under different values of the nanotube volume fractions. The natural frequencies are obtained for nonlinear problem. Numerical results reveal that the natural frequencies as well as the nonlinear to linear frequency ratios are increased by increasing the CNT volume fraction. The results also show that the natural frequencies are reduced but the nonlinear to linear frequency ratios are increased by increasing the temperature rise.

Keywords: Nonlinear oscillation, nano-composite, multi-scale approach

1. Introduction

Recently, a new member of advanced material family, carbon nanotube-reinforced composites, have been synthesized [1–3]. As the mechanical properties of composites depend directly upon the embedded fiber mechanical behavior, replacing conventional micro-sized fibers with CNTs can potentially improve composite properties, such as tensile strength and elastic modulus. Therefore, the introduction of carbon nanotubes into polymers may improve their applications in the fields of reinforcing composites, electronic devices and more.

Most studies on carbon nanotube-reinforced composites (CNTRCs) have focused on their material properties [4–9]. Several investigations have shown that the addition of small amounts of carbon nanotube can considerably improve the mechanical, electrical and thermal properties of polymeric composites [6–9]. Even though these studies are quite useful in establishing the stress– strain behavior of the nanocomposites, their use in actual structural applications is the ultimate purpose for the development of this advanced class of materials. As a result, there is a need to observe the global response of CNTRCs in an actual structural element. Wuite and Adali [10] examined the deflection and stress of nanocomposite reinforced beams using a multi-scale analysis. They found that a small percentage of nanotube reinforcement leads to significant improvements in beam stiffness. Vodenitcharova and Zhang [11] studied the pure bending and bending-induced local buckling of a nanocomposite beam reinforced by a singlewalled carbon nanotube. Shen [12] found that the nonlinear bending behavior can be considerably improved through the use of a functionally graded distribution of CNTs in the matrix. In order to increase the buckling load and postbuckling strength of CNTRC plates under a low nanotube volume fraction, the concept of functionally graded materials has been applied to the nanocomposite plates reinforced by single-walled carbon nanotubes (SWCNTs) [13,14]. They found that in some cases
the CNTRC plate with intermediate CNT volume fraction does not have intermediate buckling temperature and initial thermal postbuckling strength [14]. Moreover, Ke et al. [15] investigated the nonlinear free vibration of functionally graded CNTRC Timoshenko beams. They found that both linear and nonlinear frequencies of functionally graded CNTRC beam with symmetrical distribution of CNTs are higher than those of beams with uniform or unsymmetrical distribution of CNTs. Recently Shooshtari and Rafiee [21] studied the free and forced vibrations of clamped functionally graded beams. In their studies primary, subharmonic and superharmonic resonances of FGbeam have been investigated.

The objective of the present work is to study the nonlinear free oscillation of nanocomposite plates reinforced by the SWCNT within the framework of third order shear deformation theory and von Kármán geometric nonlinearity. The material properties of the CNTRC are assumed to be uniform in the thickness direction. The governing equations are derived by using Hamilton principle and are then solved by an improved perturbation technique to obtain the nonlinear vibration frequencies of CNTRC plates. A detailed parametric study is conducted to gain an insight into the influences of nanotube volume fraction and vibration amplitude on the nonlinear free vibration characteristics of CNTRC beams.

2. Formulations

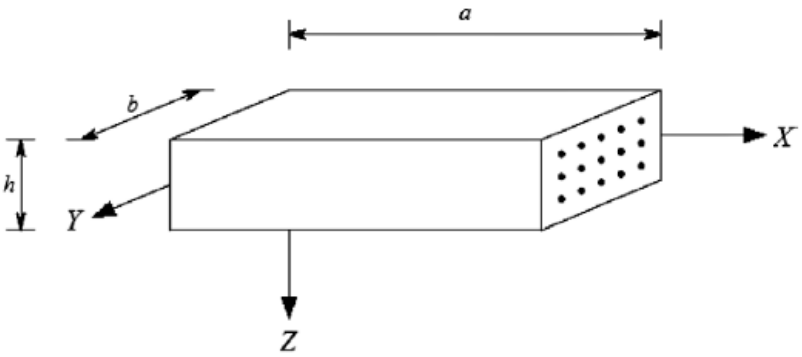

Fig 1. A
CNTRC Plate.

Consider a rectangular CNTRC plate as shown in Fig. 1. The length, width and thickness of the CNTRC plate are *a*, *b* and *h*. As usual, the coordinate system has its origin at the corner of the plate on the middle plane. Let $\bar{U}$, $\bar{V}$ and $\bar{W}$ be the plate displacements parallel to a right-hand set of axes (*X*, *Y*, *Z*), where *X* is longitudinal and *Z* is perpendicular to the plate. $\bar{\Phi}_x$ and $\bar{\Phi}_y$ are the mid-plane rotations of the normal about the *Y* and *X* axes, respectively. It is assumed that the CNTRC is made from a mixture of SWCNT and an isotropic matrix. We first determine the effective material properties of CNTRC. It was pointed out by many investigators [8,16] that the material properties of the SWCNT and CNTRC are anisotropic. According to the rule of mixture, the effective Young's modulus and shear modulus of CNTRC can be expressed as [12]

$$E_{11} = \eta_1 V_{cnt} E_{11}^{cnt} + V_m E^m \tag{1}$$

$$\frac{\eta_2}{E_{22}} = \frac{V_{cnt}}{E_{22}^{cnt}} + \frac{V_m}{E^m} \tag{2}$$

$$\frac{\eta_3}{G_{12}} = \frac{V_{cnt}}{G_{12}^{cnt}} + \frac{V_m}{G^m} \tag{3}$$

where E_{11}^{cnt}, E_{22}^{cnt} and G_{12}^{cnt} are the Young's moduli and shear modulus, respectively, of the carbon nanotube, and E_m and G_m are corresponding properties for the matrix. With the knowledge that load transfer between the nanotube and polymeric phases is less than perfect (e.g. the surface effects, strain gradients effects, intermolecular coupled stress effects, etc.), we introduced η_j (j = 1,2,3) into Eqs. (1)–(3) to consider the size-dependent material properties. η_j is called the CNT efficiency parameter which will be determined later by matching the elastic modulus of CNTRCs observed from the MD simulation results with the numerical results obtained from the rule of mixture. V_{CN} and V_m are the carbon nanotube and matrix volume fractions and are related by

$$V_m + V_{CN} = 1 \tag{4}$$

in which

$$V_{CN} = \frac{w_{CN}}{w_{CN} + \left(\rho_{CN}/\rho_m\right) - \left(\rho_{CN}/\rho_m\right) w_{CN}} \tag{5}$$

where w_{CN} is the mass fraction of nanotube, and ρ_{CN} and ρ_m are the densities of carbon nanotube and matrix, respectively. The thermal expansion coefficients in the longitudinal and transverse directions can be expressed as

$$\alpha_{11} = V_{CN}\alpha_{11}^{CN} + V_m\alpha^m \tag{6a}$$

$$\alpha_{22} = (1+\nu_{12}^{CN})V_{CN}\alpha_{22}^{CN} + (1+\nu^m)V_m\alpha^m - \nu_{12}\alpha_{11} \tag{6b}$$

where α_{11}^{CN}; α_{22}^{CN} and α^{m} are thermal expansion coefficients, and ν_{12}^{CN} and ν^{m} are Poisson's ratios, respectively, of the carbon nanotube and matrix. Poisson's ratio and mass density ρ can be calculated by

$$\nu_{12} = V_{CN}\nu_{12}^{CN} + V_m\nu^m, \quad \rho = V_{CN}\rho^{CN} + V_m\rho^m \tag{7}$$

It is assumed that the material property of nanotube and matrix is a function of temperature, so that the effective material properties of CNTRCs, like Young's modulus, shear modulus and thermal expansion coefficients, are functions of temperature and position.

A higher-order shear deformation plate theory has been developed by Reddy [17]. This theory assumes that the transverse shear strains are parabolically distributed across the plate thickness. The displacement field can be expressed as

$$\bar{U} = \bar{U}_0 + Z\left[\bar{\Phi}_x - \frac{4}{3}\left(\frac{Z}{h}\right)^2\left(\bar{\Phi}_x + \frac{\partial \bar{W}}{\partial X}\right)\right] \tag{8a}$$

$$\bar{V} = \bar{V}_0 + Z\left[\bar{\Phi}_y - \frac{4}{3}\left(\frac{Z}{h}\right)^2\left(\bar{\Phi}_y + \frac{\partial \bar{W}}{\partial Y}\right)\right] \tag{8b}$$

$$\bar{W} = \bar{W}_0 \tag{8c}$$

where $\bar{U}_0$, $\bar{V}_0$, and $\bar{W}_0$ denote the displacements of a point (x, y) on the midplane.

Thermal force resultants, thermal moment resultants and higher order thermal moment resultants due to temperature rise from the reference temperature T_0 at which there are no thermal strains, $\Delta T = T - T_0$ are defined by

$$\begin{bmatrix} \bar{N}^T & \bar{M}_x^T & \bar{P}_x^T \\ \bar{N}_y^T & \bar{M}_y^T & \bar{P}_y^T \\ \bar{N}_{xy}^T & \bar{M}_{xy}^T & \bar{P}_{xy}^T \end{bmatrix} = \int_{-h/2}^{+h/2} \begin{bmatrix} A_x \\ A_y \\ A_{xy} \end{bmatrix} \left(1, Z, Z^3\right) \Delta T dZ \tag{9}$$

$$\begin{bmatrix} \bar{S}_x^T \\ \bar{S}_y^T \\ \bar{S}_{xy}^T \end{bmatrix} = \begin{bmatrix} \bar{M}_x^T \\ \bar{M}_y^T \\ \bar{M}_{xy}^T \end{bmatrix} - \frac{4}{3h^2} \begin{bmatrix} \bar{P}_x^T \\ \bar{P}_y^T \\ \bar{P}_{xy}^T \end{bmatrix} \tag{10}$$

where

$$\begin{bmatrix} A_x \\ A_y \\ A_{xy} \end{bmatrix} = \begin{bmatrix} \bar{Q}_{11} & \bar{Q}_{12} & \bar{Q}_{16} \\ \bar{Q}_{12} & \bar{Q}_{22} & \bar{Q}_{26} \\ \bar{Q}_{16} & \bar{Q}_{26} & \bar{Q}_{66} \end{bmatrix} \begin{bmatrix} 1 & 0 \\ 0 & 1 \\ 0 & 0 \end{bmatrix} \begin{bmatrix} \alpha_{11} \\ \alpha_{22} \end{bmatrix} \tag{11}$$

and

$$Q_{11} = \frac{E_{11}}{1-\nu_{12}\nu_{21}}, \quad Q_{22} = \frac{E_{22}}{1-\nu_{12}\nu_{21}}, \quad Q_{12} = \frac{\nu_{21}E_{11}}{1-\nu_{12}\nu_{21}}, \quad Q_{16} = Q_{26} = 0, \quad Q_{66} = G_{12}, \quad Q_{44} = G_{23}, \quad Q_{55} = G_{13} \tag{12}$$

2.1. Governing Equations

Shen [19] derived a set of general von Kármán-type equations based on Reddy's higher-order shear deformation plate theory which can be expressed in terms of a transverse displacement $\bar{W}$, two rotations $\bar{\Phi}_x$ and $\bar{\Phi}_y$, and stress function F defined by Eqs. (9).

$$\bar{N}_x = \frac{\partial^2 \bar{F}}{\partial Y^2}, \quad \bar{N}_y = \frac{\partial^2 \bar{F}}{\partial X^2}, \quad \bar{N}_{xy} = -\frac{\partial^2 \bar{F}}{\partial X \partial Y} \tag{13}$$

Hence, the motion equations of a CNTRC plate, including thermal effects, can be expressed by

$$\tilde{L}_{11}\left(\bar{W}\right) - \tilde{L}_{12}\left(\bar{\Phi}_x\right) - \tilde{L}_{13}\left(\bar{\Phi}_y\right) + \tilde{L}_{14}\left(\bar{F}\right) - \tilde{L}_{15}\left(\bar{N}^T\right) - \tilde{L}_{16}\left(\bar{M}^T\right) = \tilde{L}\left(\bar{W}, \bar{F}\right) + \tilde{L}_{17}\left(\ddot{\bar{W}}\right) + I_8\left(\ddot{\bar{\Phi}}_{x,x} + \ddot{\bar{\Phi}}_{y,y}\right) + q \tag{14a}$$

$$\tilde{L}_{21}\left(\overline{F}\right)+\tilde{L}_{22}\left(\overline{\Phi}_x\right)+\tilde{L}_{23}\left(\overline{\Phi}_y\right)-\tilde{L}_{24}\left(\overline{W}\right)-\tilde{L}_{25}\left(\overline{N}^T\right)=-\frac{1}{2}\tilde{L}\left(\overline{W},\overline{W}\right) \tag{14b}$$

$$\tilde{L}_{31}\left(\overline{W}\right)+\tilde{L}_{32}\left(\overline{\Phi}_x\right)-\tilde{L}_{33}\left(\overline{\Phi}_y\right)+\tilde{L}_{34}\left(\overline{F}\right)-\tilde{L}_{35}\left(\overline{N}^T\right)-\tilde{L}_{36}\left(\overline{S}^T\right)=I_9\ddot{\overline{W}}_{,x}+I_{10}\ddot{\overline{\Phi}}_x \tag{14c}$$

$$\tilde{L}_{41}\left(\overline{W}\right)-\tilde{L}_{42}\left(\overline{\Phi}_x\right)+\tilde{L}_{43}\left(\overline{\Phi}_y\right)+\tilde{L}_{44}\left(\overline{F}\right)-\tilde{L}_{45}\left(\overline{N}^T\right)-\tilde{L}_{46}\left(\overline{S}^T\right)=I_9\ddot{\overline{W}}_{,y}+I_{10}\ddot{\overline{\Phi}}_y \tag{14d}$$

in which the linear operators $L_{ij}(\ )$ and the nonlinear operator $L(\ )$ are defined as in Shen [19].

All four edges of the plate are assumed to be simply supported with no in-plane displacements. The boundary conditions are

$x=0,a$:

$$\overline{W}=\overline{\Phi}_y=0 \tag{15a}$$

$$\overline{N}_{xy}=0 \tag{15b}$$

$$\overline{U}=0 \tag{15c}$$

$y=0,b$:

$$\overline{W}=\overline{\Phi}_x=0 \tag{16a}$$

$$\overline{N}_{xy}=0 \tag{16b}$$

$$\overline{V}=0 \tag{16c}$$

The conditions expressing the immovability conditions (15c) and (16c) are fulfilled on the average sense as [19]

$$\int_0^b\int_0^a\frac{\partial\overline{U}}{\partial X}dXdY=0 \tag{17a}$$

$$\int_0^a\int_0^b\frac{\partial\overline{V}}{\partial Y}dYdX=0 \tag{17b}$$

In Eq. (13)

$$\frac{\partial\overline{U}}{\partial X}=A_{11}^*\frac{\partial^2\overline{F}}{\partial Y^2}+A_{12}^*\frac{\partial^2\overline{F}}{\partial X^2}+\left(B_{11}^*-\frac{4}{3h^2}E_{11}^*\right)\frac{\partial\overline{\Phi}_x}{\partial X}+\left(B_{12}^*-\frac{4}{3h^2}E_{12}^*\right)\frac{\partial\overline{\Phi}_y}{\partial Y}$$
$$-\frac{4}{3h^2}\left(E_{11}^*\frac{\partial^2\overline{W}}{\partial X^2}+E_{12}^*\frac{\partial^2\overline{W}}{\partial Y^2}\right)-\frac{1}{2}\left(\frac{\partial\overline{W}}{\partial X}\right)^2-\left(A_{11}^*\overline{N}_x^T+A_{12}^*\overline{N}_y^T\right) \tag{18a}$$

$$\frac{\partial\overline{U}}{\partial V}=A_{22}^*\frac{\partial^2\overline{F}}{\partial X^2}+A_{12}^*\frac{\partial^2\overline{F}}{\partial Y^2}+\left(B_{21}^*-\frac{4}{3h^2}E_{21}^*\right)\frac{\partial\overline{\Phi}_x}{\partial X}+\left(B_{22}^*-\frac{4}{3h^2}E_{22}^*\right)\frac{\partial\overline{\Phi}_y}{\partial Y}$$
$$-\frac{4}{3h^2}\left(E_{21}^*\frac{\partial^2\overline{W}}{\partial X^2}+E_{22}^*\frac{\partial^2\overline{W}}{\partial Y^2}\right)-\frac{1}{2}\left(\frac{\partial\overline{W}}{\partial Y}\right)^2-\left(A_{12}^*\overline{N}_x^T+A_{22}^*\overline{N}_y^T\right) \tag{18b}$$

In Eqs. (18), and in what follows: $\left[A_{ij}^*\right],\left[B_{ij}^*\right],\left[D_{ij}^*\right],\left[E_{ij}^*\right],\left[F_{ij}^*\right]$ and $\left[H_{ij}^*\right]$ (i, j = 1, 2, 6) are reduced stiffness matrices, determined through relationships [18]

$$\mathbf{A}^*=\mathbf{A}^{-1},\quad \mathbf{B}^*=-\mathbf{A}^{-1}\mathbf{B},\quad \mathbf{D}^*=\mathbf{D}-\mathbf{B}\mathbf{A}^{-1}\mathbf{B},\quad \mathbf{E}^*=-\mathbf{A}^{-1}\mathbf{E}$$
$$\mathbf{F}^*=\mathbf{F}-\mathbf{E}\mathbf{A}^{-1}\mathbf{B},\quad \mathbf{H}^*=\mathbf{H}-\mathbf{E}\mathbf{A}^{-1}\mathbf{E} \tag{19}$$

where A_{ij} , B_{ij}, etc., are the plate stiffnesses, defined by

$$\left(A_{ij},B_{ij},D_{ij},E_{ij},F_{ij},H_{ij},\right)=\int_{-h/2}^{h/2}\left(Q_{ij}\right)\left(1,Z,Z^2,Z^3,Z^4,Z^6\right)dZ\quad\left(i,j=1,2,6\right) \tag{20a}$$

$$\left(A_{ij},D_{ij},F_{ij},\right)=\int_{-h/2}^{h/2}\left(Q_{ij}\right)\left(1,Z,Z^2\right)dZ\quad\left(i,j=4,5\right) \tag{20b}$$

and the inertias I_i (i = 1–5, 7) are defined by

$$\left(I_1,I_2,I_3,I_4,I_5,I_7\right)=\int_{-h/2}^{h/2}\left(Q_{ij}\right)\left(1,Z,Z^2,Z^3,Z^4,Z^6\right)dZ\quad\left(i,j=1,2,6\right) \tag{21}$$

and

$$\overline{I}_2=I_2-\frac{4}{3h^2}I_4,\quad \overline{I}_5=I_5-\frac{4}{3h^2}I_7,\quad \overline{I}_3=I_3-\frac{8}{3h^2}I_5+\frac{16}{9h^4}I_7 \tag{22}$$

$$I_8 = \frac{I_2\overline{I}_2}{I_1} - \overline{I}_3 - \frac{4}{3h^2}\overline{I}_5, \quad I_9 = \frac{4}{3h^2}\left(\overline{I}_5 - \frac{I_4\overline{I}_2}{I_1}\right), \quad I_{10} = \frac{I_2\overline{I}_2}{I_1} - \overline{I}_3$$

The following dimensionless quantities are introduced:

$$x = \pi X/a, \quad y = \pi Y/b, \quad z = Z/h, \quad \beta = a/b, \quad W = \overline{W}/\left[D_{11}^* D_{22}^* A_{11}^* A_{22}^*\right]^{1/4}$$

$$F = \overline{F}/\left[D_{11}^* D_{22}^*\right]^{1/2}, \quad \left(\Phi_x, \Phi_y\right) = \left(\overline{\Phi}_x, \overline{\Phi}_y\right) a/\pi\left[D_{11}^* D_{22}^* A_{11}^* A_{22}^*\right]^{1/4}, \quad \gamma_5 = -A_{12}^*/A_{22}^*$$

$$\gamma_{14} = \left[D_{22}^*/D_{11}^*\right]^{1/2}, \quad \gamma_{24} = \left[A_{11}^*/A_{22}^*\right]^{1/2}, \quad \left(\gamma_{T1}, \gamma_{T2}\right) = \left(A_x^T, A_y^T\right) a^2/\pi^2\left[D_{11}^*/D_{22}^*\right]^{1/2}$$

$$\left(\gamma_{T3}, \gamma_{T4}, \gamma_{T6}, \gamma_{T7}\right) = \left(D_x^T, D_y^T, F_x^T, F_y^T\right) a^2/\pi^2 h^2 D_{11}^*$$

$$\left(M_x, M_y, P_x, P_y, M_x^T, M_y^T, P_x^T, P_y^T\right) \tag{23}$$

$$= \left(\overline{M}_x, \overline{M}_y, 4\overline{P}_x/3h^2, 4\overline{P}_y/3h^2, \overline{M}_x^T, \overline{M}_y^T, 4\overline{P}_x^T/3h^2, 4\overline{P}_Y^T/3h^2\right) a^2/\pi^2 D_{11}^*\left[D_{11}^* D_{22}^* A_{11}^* A_{22}^*\right]^{1/4}$$

$$\tau = \frac{\pi t}{a}\sqrt{\frac{E_0}{\rho_0}}, \quad \gamma_{170} = -\frac{I_1 E_0 a^2}{\pi^2 \rho_0 D_{11}^*}, \quad \gamma_{171} = -\frac{4E_0\left(I_5 I_1 - I_4 I_2\right)}{3\rho_0 h^2 I_1 D_{11}^*}$$

$$\left(\gamma_{80}, \gamma_{90}, \gamma_{10}\right) = \left(I_8, I_9, I_{10}\right)\frac{E_0}{\rho_0 D_{11}^*}, \quad \lambda_q = qa^4/\pi^4 D_{11}^*\left[D_{11}^* D_{22}^* A_{11}^* A_{22}^*\right]^{1/4}$$

in which E_0 and ρ_0 are the reference values of E_m and ρ_m at the room temperature (T_0=300 K), respectively, and $A_x^T\left(=A_y^T\right)$, $D_x^T\left(=D_y^T\right)$ and $F_x^T\left(=F_y^T\right)$ are defined by

$$\begin{bmatrix} A_x^T & D_x^T & F_x^T \\ A_y^T & D_y^T & F_y^T \end{bmatrix}\Delta T = -\int_{-h/2}^{h/2}\begin{bmatrix} A_x \\ A_y \end{bmatrix}\Delta T\left(Z\right)\left(1, Z, Z^2\right) dZ \tag{24}$$

From Eq. (24), A_x^T, D_x^T and F_x^T are determined. Eqs. (14a-d) can then be re-written in the following dimensionless form

$$\tilde{L}_{11}\left(\overline{W}\right) - \tilde{L}_{12}\left(\overline{\Phi}_x\right) - \tilde{L}_{13}\left(\overline{\Phi}_y\right) + \tilde{L}_{14}\left(\overline{F}\right) - \tilde{L}_{15}\left(\overline{N}^T\right) - \tilde{L}_{16}\left(\overline{M}^T\right) = \tilde{L}\left(\overline{W}, \overline{F}\right) + \tilde{L}_{17}\left(\ddot{\overline{W}}\right) - \overline{I}_{17}\left(\ddot{\overline{\Phi}}_{x,x} + \ddot{\overline{\Phi}}_{y,y}\right) + q \tag{25a}$$

$$\tilde{L}_{21}\left(\overline{F}\right) + \tilde{L}_{22}\left(\overline{\Phi}_x\right) + \tilde{L}_{23}\left(\overline{\Phi}_y\right) - \tilde{L}_{24}\left(\overline{W}\right) - \tilde{L}_{25}\left(\overline{N}^T\right) = \frac{1}{2}\tilde{L}\left(\overline{W}, \overline{W}\right) \tag{25b}$$

$$\tilde{L}_{31}\left(\overline{W}\right) + \tilde{L}_{32}\left(\overline{\Phi}_x\right) - \tilde{L}_{33}\left(\overline{\Phi}_y\right) + \tilde{L}_{34}\left(\overline{F}\right) - \tilde{L}_{35}\left(\overline{N}^T\right) - \tilde{L}_{36}\left(\overline{S}^T\right) = I_9\ddot{\overline{W}}_{,x} + I_{10}\ddot{\overline{\Phi}}_x \tag{25c}$$

$$\tilde{L}_{41}\left(\overline{W}\right) - \tilde{L}_{42}\left(\overline{\Phi}_x\right) + \tilde{L}_{43}\left(\overline{\Phi}_y\right) + \tilde{L}_{44}\left(\overline{F}\right) - \tilde{L}_{45}\left(\overline{N}^T\right) - \tilde{L}_{46}\left(\overline{S}^T\right) = I_9\ddot{\overline{W}}_{,y} - I_{10}\ddot{\overline{\Phi}}_y \tag{25d}$$

The boundary conditions of Eqs. (15,16) become

$x = 0, \pi$:

$$W = \Phi_y = 0 \tag{26a}$$

$$F_{,xy} = 0 \tag{26b}$$

$$\int_0^\pi\int_0^\pi\left[\gamma_{24}^2\beta^2\frac{\partial^2 F}{\partial y^2} - \gamma_5\frac{\partial^2 F}{\partial x^2} + \gamma_{24}\left(\gamma_{511}\frac{\partial\Phi_x}{\partial x} + \gamma_{233}\frac{\partial\Phi_y}{\partial y}\right) - \gamma_{24}\left(\gamma_{611}\frac{\partial^2 W}{\partial x^2} + \gamma_{244}\beta^2\frac{\partial^2 W}{\partial y^2}\right) - \frac{1}{2}\gamma_{24}\beta^2\left(\frac{\partial W}{\partial y}\right)^2 + \left(\gamma_{T2} - \gamma_5\gamma_{T1}\right)\Delta T\right] dxdy = 0 \tag{26c}$$

$y = 0, \pi$:

$$W = \Phi_y = 0 \tag{27a}$$

$$F_{,xy} = 0 \tag{27b}$$

$$\int_0^{\pi}\int_0^{\pi}\left[\frac{\partial^2 F}{\partial x^2}-\gamma_5\beta^2\frac{\partial^2 F}{\partial y^2}+\gamma_{24}\left(\gamma_{220}\frac{\partial\Phi_x}{\partial x}+\gamma_{522}\frac{\partial\Phi_y}{\partial y}\right)-\gamma_{24}\left(\gamma_{240}\frac{\partial^2 W}{\partial x^2}+\gamma_{622}\beta^2\frac{\partial^2 W}{\partial y^2}\right)\right.$$
$$\left.-\frac{1}{2}\gamma_{24}\beta^2\left(\frac{\partial W}{\partial y}\right)^2+\left(\gamma_{T2}-\gamma_5\gamma_{T1}\right)\Delta T\right]dxdy=0 \tag{27c}$$

3. Solution Methodology

We assume that the solutions of Eqs. (25a-d) can be expressed as

$$\begin{aligned}
W(x,y,\tau)&=\underline{W}(x,y)+\hat{W}(x,y,\tau)\\
\Phi_x(x,y,\tau)&=\underline{\Phi}_x(x,y)+\hat{\Phi}_x(x,y,\tau)\\
\Phi_y(x,y,\tau)&=\underline{\Phi}_y(x,y)+\hat{\Phi}_y(x,y,\tau)\\
F(x,y,\tau)&=\underline{F}(x,y)+\hat{F}(x,y,\tau)
\end{aligned} \tag{28}$$

where $\underline{W}(x,y)$ is an initial thermo-mechanical deflection due to initial thermal bending moment, and $\hat{W}(x,y,\tau)$ is an additional deflection. $\underline{\Phi}_x(x,y)$, $\underline{\Phi}_y(x,y)$ and $\underline{F}(x,y)$ are the mid-plane rotations and stress function corresponding to $\underline{W}(x,y)$. $\hat{\Phi}_x(x,y,\tau)$, $\hat{\Phi}_y(x,y,\tau)$ and $\hat{F}(x,y,\tau)$ are defined analogously to $\underline{\Phi}_x(x,y)$, $\underline{\Phi}_y(x,y)$ and $\underline{F}(x,y)$, but is for $\hat{W}(x,y,\tau)$.

For the pre-vibration solutions $\underline{W}(x,y)$, $\underline{\Phi}_x(x,y)$, $\underline{\Phi}_y(x,y)$ and $\underline{F}(x,y)$, the same methodology of the [20] can be followed.

Then an initially stressed CNTRC plate is under consideration and $\hat{W}(x,y,\tau)$, $\hat{\Phi}_x(x,y,\tau)$, $\hat{\Phi}_y(x,y,\tau)$ and $\hat{F}(x,y,\tau)$ satisfy the nonlinear equations

$$\begin{aligned}
&L_{11}(\hat{W})-L_{12}(\hat{\Phi}_x)-L_{13}(\hat{\Phi}_y)+\gamma_{14}L_{14}(\hat{F})\\
&=\gamma_{14}\beta^2 L\left(\hat{W}+\underline{W},\hat{F}\right)+L_{17}\left(\ddot{\hat{W}}\right)+\gamma_{80}\left(\ddot{\hat{\Phi}}_{x,x}+\beta\ddot{\hat{\Phi}}_{y,y}\right)+\lambda_q
\end{aligned} \tag{29a}$$

$$L_{21}(\hat{F})+\gamma_{24}L_{22}(\hat{\Phi}_x)+\gamma_{24}L_{23}(\hat{\Phi}_y)-\gamma_{24}L_{24}(\hat{W})=-\frac{1}{2}\gamma_{24}\beta^2 L\left(\hat{W}+2\underline{W},\hat{W}\right) \tag{29b}$$

$$L_{31}(\hat{W})+L_{32}(\hat{\Phi}_x)-L_{33}(\hat{\Phi}_y)+\gamma_{14}L_{34}(\hat{F})=\gamma_{90}\ddot{\hat{W}}_{,x}+\gamma_{10}\ddot{\hat{\Phi}}_x \tag{29c}$$

$$L_{41}(\hat{W})+L_{42}(\hat{\Phi}_x)-L_{43}(\hat{\Phi}_y)+\gamma_{14}L_{44}(\hat{F})=\gamma_{90}\beta\ddot{\hat{W}}_{,y}+\gamma_{10}\ddot{\hat{\Phi}}_y \tag{29d}$$

The initial conditions are assumed to be

$$\tilde{W}\Big|_{\tau=0}=\left.\frac{\partial\tilde{W}}{\partial\tau}\right|_{\tau=0}=0 \tag{30a}$$

$$\hat{\Phi}_x\Big|_{\tau=0}=\left.\frac{\partial\hat{\Phi}_x}{\partial\tau}\right|_{\tau=0}=0 \tag{30b}$$

$$\hat{\Phi}_y\Big|_{\tau=0}=\left.\frac{\partial\hat{\Phi}_y}{\partial\tau}\right|_{\tau=0}=0 \tag{30c}$$

A perturbation technique is now used to solve Eqs. (29a-d). The essence of this procedure, in the present case, is to assume that

$$\begin{aligned}
\hat{W}(x,y,\tilde{\tau},\varepsilon) &= \sum_{j=1}\varepsilon^j \hat{W}_j(x,y,\tilde{\tau}) \\
\hat{F}(x,y,\tilde{\tau},\varepsilon) &= \sum_{j=0}\varepsilon^j \hat{F}_j(x,y,\tilde{\tau}) \\
\hat{\Phi}_x(x,y,\tilde{\tau},\varepsilon) &= \sum_{j=1}\varepsilon^j \hat{\Phi}_{xj}(x,y,\tilde{\tau}) \\
\hat{\Phi}_y(x,y,\tilde{\tau},\varepsilon) &= \sum_{j=1}\varepsilon^j \hat{\Phi}_{yj}(x,y,\tilde{\tau}) \\
\lambda_q(x,y,\tilde{\tau},\varepsilon) &= \sum_{j=1}\varepsilon^j \lambda_j(x,y,\tilde{\tau})
\end{aligned} \tag{31}$$

where ε is a small perturbation parameter. Here we introduce an important parameter $\tilde{\tau} = \varepsilon\tau$, which may be called a slow variable, to improve perturbation procedure for solving nonlinear dynamic problem. Substituting Eq. (31) into Eqs. (29a-d), and collecting terms of the same order of ε, a set of perturbation equations is obtained. Applying Galerkin procedure to the second equation of each order, and solving these equations step by step, we obtain asymptotic solutions, up to third-order, as

$$\begin{aligned}
&\tilde{W}(x,y,\tau) = \varepsilon\left[w_1(\tau) + g_1\ddot{w}_1(\tau)\right]\sin mx\,\sin ny + \left(\varepsilon w_1(\tau)\right)^3 \\
&\left[\alpha g_{311}\sin mx\,\sin ny + g_{331}\sin 3mx\,\sin ny + g_{313}\sin mx\,\sin 3ny\right] + O\left(\varepsilon^4\right)
\end{aligned} \tag{32}$$

$$\begin{aligned}
&\hat{\Phi}_x(x,y,\tau) = \varepsilon\left[g_{11}^{(1'1)}w_1(\tau) + g_2\ddot{w}_1(\tau)\right]\cos mx\sin ny + g_{12}\left(\varepsilon w_1(\tau)\right)^2\sin 2mx + \\
&\left(\varepsilon w_1(\tau)\right)^3\left[\begin{matrix}\alpha g_{11}^{(1'1)}g_{311}\cos mx\sin ny + g_{11}^{(3'1)}g_{331}\cos 3mx\sin ny + g_{11}^{(1'3)} \\ g_{313}\cos mx\sin 3ny\end{matrix}\right] + O\left(\varepsilon^4\right)
\end{aligned} \tag{33}$$

$$\begin{aligned}
&\hat{\Phi}_y(x,y,\tau) = \varepsilon\left[g_{21}^{(1'1)}w_1(\tau) + g_3\ddot{w}_1(\tau)\right]\sin mx\cos ny + g_{22}\left(\varepsilon w_1(\tau)\right)^2\sin 2ny + \\
&\left(\varepsilon w_1(\tau)\right)^3\left[\begin{matrix}\alpha g_{21}^{(1'1)}g_{311}\sin mx\cos ny + g_{21}^{(3'1)}g_{331}\sin 3mx\cos ny + g_{21}^{(1'3)} \\ g_{313}\sin mx\cos 3ny\end{matrix}\right] + O\left(\varepsilon^4\right)
\end{aligned} \tag{34}$$

$$\begin{aligned}
&\tilde{F}(x,y,\tau) = \varepsilon\left[g_{31}^{(1'1)}w_1(\tau) + g_4\ddot{w}_1(\tau)\right]\sin mx\,\sin ny - \left(\varepsilon w_1(\tau)\right)^2 \\
&\times\left(B_{00}^{(2)}y^2/2 + b_{00}^{(2)}x^2/2 - g_{402}\cos 2ny - g_{420}\cos 2mx\right) \\
&+\left(\varepsilon w_1(\tau)\right)^3\left[\begin{matrix}\alpha g_{31}^{(1'1)}g_{311}\sin mx\,\sin ny + g_{311}^{(3'1)}g_{331}\sin 3mx\,\cos ny + g_{31}^{(1'3)} \\ g_{313}\sin mx\,\sin 3ny\end{matrix}\right] + O\left(\varepsilon^4\right)
\end{aligned} \tag{35}$$

$$\begin{aligned}
&\lambda_q(x,y,\tau) = \varepsilon\left[g_{41}w_1(\tau) + g_{43}\ddot{w}_1(\tau)\right]\sin mx\sin ny + \left(\varepsilon w_1(\tau)\right)^2\left(g_{441}\cos 2mx + g_{442}\cos 2ny\right) \\
&-\gamma_{14}\beta^2\left(\varepsilon w_1(\tau)\right)^2\sum_k\sum_l w_{kl}\times\left(B_{00}^{(2)}k^2 + b_{00}^{(2)}l^2 - 4k^2n^2g_{402}\cos 2ny - 4l^2m^2g_{420}\cos 2mx\right)\sin kx\sin ly \\
&+\bar{\alpha}g_{42}\left(\varepsilon w_1(\tau)\right)^3 + \sin mx\sin ny + O\left(\varepsilon^4\right)
\end{aligned} \tag{36}$$

Note that in Eqs. (32)–(36) $\tilde{\tau}$ is replaced by τ and for the case of free vibration $\alpha = 0$, $\bar{\alpha} = 1$, otherwise $\alpha = 1$, $\bar{\alpha} = 0$. Coefficients $g_{11}^{(i,j)}$, $g_{21}^{(i,j)}$, $g_{31}^{(i,j)}$ (i, j = 1, 3) etc. are given in detail in [22]. Multiplying Eq. (36) by (sin *mx* sin *ny*) and integrating over the plate area, one has

$$g_{43}\frac{d^2\left(\varepsilon w_1\right)}{d\tau^2} + g_{41}\left(\varepsilon w_1\right) + g_{44}\left(\varepsilon w_1\right)^2 + \bar{\alpha}g_{42}\left(\varepsilon w_1\right)^3 = \bar{\lambda}_q(\tau) \tag{37}$$

in which

$$\bar{\lambda}_q(\tau) = \frac{4}{\pi^2}\int_0^\pi\int_0^\pi \lambda_q(x,y,\tau)\sin mx\sin ny dxdy \tag{38}$$

When $\bar{\alpha} = 1$, $\lambda_q = 0$ Eq. (37) becomes the free vibration equation of the plate. The nonlinear frequency of the plates can be expressed as (Wang, 1992)

$$\frac{\omega_{NL}}{\omega_L} = \sqrt{1 + \frac{9g_{42}g_{41} - 10g_{44}^2}{12g_{41}^2}\left(\frac{W_{\max}}{h}\right)^2} \tag{38}$$

where $\omega_L=(g_{41}/g_{43})^{1/2}$ is the dimensionless linear frequency.

4. Numerical Results and Discussion

Table 2 compares the dimensionless linear fundamental frequencies $\bar{\omega}=\Omega a\sqrt{\rho/E}$ of simply supported CNTRC plates. Here PmPV material is considered. The parameters used in this example are ρ^m = 1150 kg/m^3, ν^m = 0.34, α^m =45(1+0.0005ΔT) ×10^{-6}/K and E^m = (3.52-0.0034T) GPa, in which $T = T_0 + \Delta T$ andT_0 = 300 K (room temperature). The (10,10) SWCNTs are selected as reinforcements.

Material properties and effective thickness of SWCNTs used for analysis are properly chosen in the present paper by MD simulations. Typical results are listed in Table 1 [14].

For verification of the results finite element code ANSYS is used. SOLID46 element is used for the specified duty. A total number of 91204 nodes and 67500 elements are used for validation.

Table 3 shows the effects of temperature change (T = 300 and 500 K) and CNT volume fraction V_{CN}^* (= 0.12, 0.17 and 0.28) on the natural frequencies of CNTRC square plates (a/b = 1, b/ h = 20, h = 2 mm). It can be seen that the natural frequency of the CNTRC plate decreases with increase in temperature rise, but increases with increase in the CNT volume fraction V_{CN}^*.

Table 1. Temperature-dependent material properties for (10,10) SWCNT (L = 9.26 nm, R = 0.68 nm, h = 0.067 nm, ν_{12}^m, ρ^{CN} = 1400 kg/m^3) (from Shen and Zhang [14]).

Temperature (K)	E_{11}^{cnt} (TPa)	E_{22}^{cnt} (TPa)	G_{12}^{cnt} (TPa)	α_{11}^{cnt} (×10^{-6} /K)	α_{22}^{cnt} (×10^{-6} /K)
300	5.6466	7.0800	1.9445	3.4584	5.1682
500	5.5308	6.9348	1.9643	4.5361	5.0189
700	5.4744	6.8641	1.9644	4.6677	4.8943
1000	5.2814	6.6220	1.9451	4.2800	4.7532

Table 2. Comparison of linear frequency $\bar{\omega}=\Omega a\sqrt{\rho/E}$ for an isotropic square plate (a/b = 1.0, b/h = 20, ν = 0.3).

	$\bar{\omega}_1$	$\bar{\omega}_2$	$\bar{\omega}_3$	$\bar{\omega}_4$	$\bar{\omega}_5$
Present	0.2849	0.7091	1.1156	1.3998	1.7854
FEM (ANSYS)	0.2906	0.7233	1.1379	1.4277	1.8211

Table 3. Effects of temperature and CNT volume fraction V_{CN}^* on the natural frequency $\bar{\Omega}=\Omega\left(a^2/h\right)\sqrt{\rho_0/E_0}$ for CNTRC square plates (a/b = 1, b/h = 20, h = 2 mm).

Temperature (K)	V_{CN}^*	Source	$\bar{\omega}_1$	$\bar{\omega}_2$	$\bar{\omega}_3$	$\bar{\omega}_4$
300	0.12	Present	15.6887	20.0896	31.2861	43.0933
		FEM	16.0025	20.4914	31.9118	43.9552
	0.17	Present	19.2201	25.1691	39.9455	55.6789
		FEM	19.6045	25.6725	40.7444	56.7925
	0.28	Present	22.9428	28.4703	43.1028	58.3540
		FEM	23.4017	29.0397	43.9649	59.5211
500	0.12	Present	10.8237	14.4169	22.4518	30.9250
		FEM	11.0402	14.7052	22.9008	31.5435
	0.17	Present	13.6291	18.4006	29.2033	40.7056
		FEM	13.9017	18.7686	29.7873	41.5197
	0.28	Present	15.1898	19.8849	30.1049	40.7570
		FEM	15.4936	20.2826	30.7070	41.5721

Table 4. Effect of ratio b/h on nonlinear frequency ratio $\bar{\Omega}/\Omega$ of CNTRC plates ($V_{CN}^*=0.12$, a/b = 1.0, ν = 0.3).

b/h	$\bar{\Omega}$	$\bar{W}_{\max}/h$				
		0.1	0.2	0.3	0.4	0.5
10	0.5773	1.0154	1.0605	1.1318	1.2251	1.3381

20	0.2849	1.0061	1.0242	1.0536	1.0933	1.1422
50	0.1184	1.0022	1.0219	1.0211	1.0600	1.0987

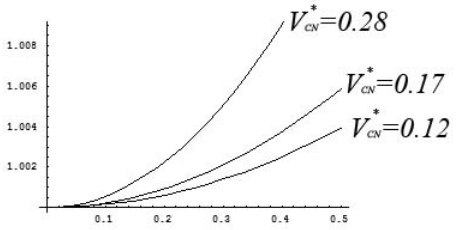

Fig. 3. The effect of CNT volume fraction on the frequency–amplitude curves of CNTRC plates. The vertical axis represent the nonlinear to linear ratio and the horizontal axis represents the $\bar{W}_{\max} / h$.

5. Conclusion

The nonlinear vibrations for simply supported CNTRC plates in thermal environments have been presented. Temperature-dependent material properties are taken into account. The formulations are based on higher-order shear deformation plate theory and general von Karman-type equations, and include thermal effects. Analytical solutions have been presented by using an improved perturbation technique. A parametric study for CNTRC plates with different values of volume fraction index and under different sets of thermal environmental conditions has been carried out. Numerical results show that the natural frequencies as well as the nonlinear to linear frequency ratios are increased by increasing the CNT volume fraction. The results also show that the natural frequencies are reduced but the nonlinear to linear frequency ratios are increased by increasing the temperature rise or by decreasing the foundation stiffness. The results confirm that a functionally graded reinforcement has a significant effect on the nonlinear vibration behavior of CNTRC plates.

References

[1]. Lau KT, Gu C, Gao GH, Ling HY, Reid SR. Stretching process of single- and multiwalled carbon nanotubes for nanocomposite applications. Carbon 2004;42:426–8.

[2]. Esawi AMK, Farag MM. Carbon nanotube reinforced composites: potential and current challenges. Mater Des 2007;28:2394–401.

[3]. Thostenson ET, Ren Z, Chou TW. Advances in the science and technology of carbon nanotubes and their composites: a review. Compos Sci Technol 2001;61:1899–912.

[4]. Odegard GM, Gates TS, Wise KE, Park C, Siochi EJ. Constitutive modelling of nanotube-reinforced polymer composites. Compos Sci Technol 2003;63:1671–87.

[5]. Hu N, Fukunaga H, Lu C, Kameyama M, Yan B. Prediction of elastic properties of carbon nanotube reinforced composites. Proce Royal Soc A 2005;461: 1685–710.

[6]. Fidelus JD, Wiesel E, Gojny FH, Schulte K, Wagner HD. Thermo-mechanical properties of randomly oriented carbon/epoxy nanocomposites. Compos Part A 2005;36:1555–61.

[7]. Bonnet P, Sireude D, Garnier B, Chauvet O. Thermal properties and percolation in carbon nanotube–polymer composites. J Appl Phys 2007;91:201910.

[8]. Han Y, Elliott J. Molecular dynamics simulations of the elastic properties of polymer/carbon nanotube composites. Comput Mater Sci 2007;39:315–23.

[9]. Zhu R, Pan E, Roy AK. Molecular dynamics study of the stress–strain behavior of carbon-nanotube reinforced Epon 862 composites. Mater Sci Eng A 2007;447:51–7.

[10]. Wuite J, Adali S. Deflection and stress behaviour of nanocomposite reinforced beams using a multiscale analysis. Compos Struct 2005;71:388–96.

[11]. Vodenitcharova T, Zhang LC. Bending and local buckling of a nanocomposite beam reinforced by a single-walled carbon nanotube. Int J Solids Struct 2006;43:3006–24.

[12]. H.-S. Shen, Nonlinear bending of functionally graded carbon nanotubereinforced composite plates in thermal environmentsCompos. Struct. 91 (2009) 9.

[13]. H.-S. Shen, Z.H. Zhu, Comput. Mater. Continua 18 (2010) 155.

[14]. H.-S. Shen, C.-L. Zhang, Mater. Des. 31 (2010) 3403.

[15]. L.-L. Ke, J. Yang, S. Kitipornchai, Compos. Struct. 92 (2010) 676.

[16]. Zhang CL, Shen HS. Temperature-dependent elastic properties of single-walled carbon nanotubes: prediction from molecular dynamics simulation. Appl Phys Lett 2006;89:081904.

[17]. Reddy, J.N., A refined nonlinear theory of plates with transverse shear deformation. International Journal of Solids and Structures 20 (1984) 881–896.

[18]. Shen, H.-S., Kármán-type equations for a higher-order shear deformation plate theory and its use in the thermal postbuckling analysis, Applied Mathematics and Mechanics 18, (1997)1137–1152.

[19]. Shen, H.-S., Nonlinear bending response of functionally graded plates subjected to transverse loads and in thermal environments. International Journal of Mechanical Sciences 44, (2002)561–584.

[20]. Yang, J., Huang, X-L., Nonlinear transient response of functionally graded plates with general imperfections in thermal environments, Comput. Methods Appl. Mech. Engrg. 196 (2007) 2619–2630.

[21]. Shooshtari A., Rafiee, M., Nonlinear forced vibration analysis of clamped functionally graded beams, accepted manuscript, Acta Mechanica, DOI 10.1007/s00707-011-0491-1.

[22]. Huang XL, Shen HS. Nonlinear vibration and dynamic response of functionally graded plates in thermal environments, International Journal of Solids and Structures 41 (2004) 2403–2427.